energy&fuels

pubs.acs.org/EF Article

Tracking Elemental Composition through Hydrotreatment of an Upgraded Pyrolysis Oil Blended with a Light Gas Oil

Rebecca L. Ware, Ryan P. Rodgers, Alan G. Marshall, Ofei D. Mante, David C. Dayton, Sylvain Verdier, Jostein Gabrielsen, and Steven M. Rowland*

Cite This: *Energy Fuels* 2020, 34, 16181−16186

ABSTRACT: The physical properties of crude bio-oils preclude their direct use as fuel. Specifically, their high oxygen content results in undesirable acidity and poor thermal stability. Therefore, the removal of oxygen is essential for the use of bio-oils as fuel. Currently, the most straightforward method for application of bio-oil as fuel is through blending with petroleum feeds. Emulsions have been explored extensively for the introduction of polar bio-oils into nonpolar petroleum feeds. Coprocessing of deoxygenated oils and petroleum feeds by fluid catalytic cracking (FCC) is another method for blending bio-oil with petroleum. Because the deoxygenated oil is less polar, it can be directly added to a petroleum feed, after which the blend is processed by FCC to further reduce the oxygen content and crack larger hydrocarbons. Here, a hydrodeoxygenated bio-oil (HDO bio-oil) is blended with a light gas oil (LGO) and then hydrotreated. The oil is characterized at each step throughout the blending process by Fourier transform ion cyclotron resonance (FT-ICR) mass spectrometry (MS) and two-dimensional gas chromatography (GCxGC) MS. FT-ICR MS showed no changes in elemental compositions resulting from the blending processes. After hydrotreating the blend, there is a reduction in the carbon number and double-bond equivalents (DBE = number of rings plus double bonds to carbon) as well as the removal of sulfur and oxygen species. GCxGC MS showed that the alkanes in the blend and hydrotreated blend are contributed by the LGO, whereas cycloalkanes originate from the HDO bio-oil. Removing oxygenated species and reducing DBE of the HDO bio-oil through blending and hydrotreatment provide an oil with a composition suitable as fuel.

INTRODUCTION

The high oxygen content of crude pyrolysis bio-oil results in high acidity and viscosity, and the low heating value and thermal stability limit its application as a replacement for petroleum fuel. Catalytic hydrotreatment is a common method for improving the bio-oil properties by removing oxygen, but it does not reduce the oxygen content enough for direct application as a fuel additive. To mitigate this problem, bio-oils are typically blended with petroleum feeds for coprocessing.[1]

The immiscibility of polar bio-oils and nonpolar petroleum feeds can be circumvented by forming emulsions to allow for blending.[2] These emulsions, however, are not inherently stable and therefore require emulsifiers and cosurfactants.[3−5] Ikura et al.[4] found that higher emulsifier concentration and energy input (stirring) during production produced more stable emulsions but at a significant cost. The use of a cosurfactant to stabilize bio-oil in diesel emulsions was shown by de Luna et al.,[6] who found that the addition of an alcohol cosurfactant stabilized higher proportions of bio-oil in diesel while using less emulsifier. The cosurfactant reduced the density difference between the continuous and droplet phases, allowing for the formation of micelles, improving the stability, and reducing the viscosity of the emulsion. Martin et al.[7] compared the emulsion stability of fast pyrolysis bio-oil and catalytic fast pyrolysis (CFP) oil when mixed with diesel. They found that the emulsion vastly improved the properties compared to the bio-oil; however, the presence of levoglucosan and char solids caused instability and phase separation of the blend. They also found that the formation of an emulsion was not necessary to blend CFP oil with diesel because most CFP components are miscible with the nonpolar diesel. Emulsions are undesirable because they are not cost-efficient and are not stable over long periods of time.

Deoxygenated bio-oils can be directly mixed with petroleum feeds and further coprocessed to produce fuels without the concerns associated with emulsions. Fluid catalytic cracking (FCC) commonly used in the petroleum industry to convert heavy molecules into smaller fuel molecules has recently been explored as a method for coprocessing bio-oils and petroleum feeds.[8−13] Fogassy et al.[11,12] showed no change in gasoline yields for a coprocessed deoxygenated bio-oil with a vacuum gas oil (VGO) versus pure VGO. The coprocessed FCC oil had lower oxygen content and higher aromatic hydrocarbon content; however, complete deoxygenation was not achieved because residual phenols were found in the coprocessed oil.[9] It was also shown, by two-dimensional gas chromatography

Received: July 24, 2020
Revised: November 18, 2020
Published: December 7, 2020

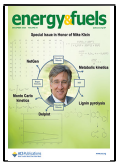

https://dx.doi.org/10.1021/acs.energyfuels.0c02437
Energy Fuels 2020, 34, 16181−16186

(GCxGC) mass spectrometry (MS), that coprocessing enhanced branched paraffins and short alkyl-chain benzene derivatives relative to FCC of VGO. When coprocessing an 80:20 mix of VGO and crude bio-oil, Ibarra et al.[13] measured higher gasoline yield that contained more naphthenes, paraffins, and olefins. The oxygenates in the product oil were attributed to the competitive adsorption of different oxygen species and hydrocarbons on the catalyst. The effect of oxygenated bio-oil model compounds on the products of FCC coprocessed feeds was explored by Jarvis et al.,[8] who found that adding oxygenated compounds to VGO and kerosene feeds had minimal effects on the liquid hydrocarbon yield and composition, with all oxygen functionalities converted. However, adding oxygen compounds increased the coke yield, consistent with other bio-oil/FCC feed coprocessing studies.[9,12]

Here, we implement GCxGC MS and Fourier transform ion cyclotron resonance mass spectrometry (FT-ICR MS) to analyze a light gas oil (LGO) and upgraded bio-oil [hydrodeoxygenated (HDO) bio-oil] through blending and hydrotreatment of the blend. GCxGC MS provides compound class identification, whereas FT-ICR MS provides elemental compositions and detection of the HDO bio-oil, which contains components that are not GC-amenable.

EXPERIMENTAL METHODS

HDO Bio-Oil Production. Methods for bio-oil production are described elsewhere.[14] Briefly, CFP of red oak in RTI's 1 ton per day plant was used to produce a hydrocarbon-rich biocrude intermediate with ~25 wt % oxygen. This biocrude was then hydrotreated with a commercially available sulfided NiMo catalyst (Haldor Topsoe A/S) in RTI's once-through down-flow trickle-bed hydrotreating pilot plant.[15] The upgraded biocrude is what is referred to as the HDO bio-oil and has less than 5 wt % oxygen. Detailed characterization of the physical and chemical properties of the red oak biocrude and hydrotreated products has been presented by Ware et al.[14]

HDO Bio-Oil and LGO Blending. The HDO bio-oil and LGO were blended in a 30:70 ratio in a 20 L heated tank at 40−50 °C to achieve an oxygen wt % of 1 by elemental analysis.

Blend Hydrotreatment. Hydrotreatment of the blend was conducted in Haldor Topsoe's once-through down-flow trickle-bed pilot plant that consists of two reactors in series.[15] The reactor effluent is separated in a high-pressure separator where the liquid effluent from the high-pressure separator is sent to a low-pressure separator and further stripped with nitrogen for removal of gases and noncondensed light hydrocarbons. The exit gases from the separators and the stripper are combined prior to sampling. Once-through pure hydrogen is used. The catalyst is diluted with an inert material (SiC mesh 60) with a 60/40 ratio and sulfided with H_2S in H_2 (10 vol %) for over 18 h at 8 bar. The total flow of the gas mixture corresponded with 550 mL/h per liter of catalyst. For hydrotreatment, the hydrogen pressure was 70 bar; the liquid hourly space velocity was 0.6 h^{-1}; the weighted-average bed temperature was 330 °C; and the ratio of H_2 to oil was 500 NL/L.

GC×GC MS. Two-dimensional gas chromatography using time-of-flight MS detection was performed as described elsewhere.[16] 1 μL of a 30 mg/mL solution of each sample in dichloromethane was injected with a split ratio of 1:5 and a gas chromatograph inlet temperature of 300 °C. The first oven temperature was set at 40 °C for 4 min before ramping to 340 °C at a rate of 3 °C/min and held for 10 min. The second column was set 5 °C higher than the first and followed the same temperature increase profile. The modulator offset was +10 °C with a modulation period of 6 s and a hot pulse of 0.8 s. The data was acquired and processed with ChromaTOF software (version 4.50) from LECO Corp. NIST libraries of model compounds were used to assign possible structures based on a similarity of >85% in the fragmentation patterns.

FT-ICR MS. All samples were dissolved in toluene at a concentration of 100 μg/mL (HPLC grade, JT Baker, Phillipsburg NJ) for positive-ion (+) atmospheric pressure photoionization (APPI) FT-ICR MS analysis with a custom built 9.4 T FT-ICR mass spectrometer described elsewhere.[17−21] A Thermo Scientific APPI source generated ions with a krypton lamp that emits 10.0 and 10.6 eV photons, a nebulizer temperature of 300 °C, sheath gas of 60 p.s.i., auxiliary gas flow of ~4 L/min, and a sample flow rate of 50 μL/min. One hundred ~6 s time-domain transients were coadded for each spectrum. Mass spectral calibration based on homologous series within each sample was performed with Predator software, and formula assignments and imaging were conducted with PetroOrg.[18,22] Magnitude-mode resolving power was ~1,300,000 at m/z 300 (center of distribution) for the hydrotreated oil, ~1,700,000 at m/z 240 for the blended oil, ~1,400,000 at m/z 290 for the hydrotreated blend, ~1,500,000 at m/z 260 for the original LGO, and ~1,200,000 at m/z 315 for the hydrotreated LGO. Note that the abundances in each double-bond equivalent (DBE) versus carbon number plot are reported relative to the individual class, not the sample as a whole.

RESULTS AND DISCUSSION

FT-ICR MS of Individual Feeds. The hydrotreated bio-oil (HDO bio-oil) has been previously characterized and compared to the original crude bio-oil.[14] That work showed a significant decrease in oxygenated species, from 42 to 5 wt %, so mixing the HDO bio-oil with LGO could be achieved without forming an emulsion. Each component was analyzed prior to blending to establish the initial baseline compositions. The FT-ICR MS-derived heteroatom class distributions for HDO bio-oil, original LGO (LGO-O), and hydrotreated LGO (LGO-H) show higher relative abundance of the hydrocarbon and S_1 classes for the LGO-O compared to the HDO bio-oil (Figure 1). In contrast, the HDO bio-oil contains a higher relative abundance of oxygen-containing heteroatom classes, O_1−O_4, as expected from the incomplete deoxygenation of the original bio-crude. The LGO-O contains O_x and S_1 species that are all removed by hydrotreatment (LGO-H). The O_x species with high relative abundance in the LGO are due to contaminants in the solvents. These contaminants have a greater effect on the LGO than on the HDO bio-oil because of the low ionization efficiency of saturated hydrocarbons, the main component in LGO based on (+) APPI.

Oxygenated contaminants identified in the blank correspond to areas of high relative abundance in the LGO plots and therefore overshadow the LGO components of interest; however, some of the LGO components can still be identified. Figure 2 shows the compositional coverage visualized by DBE

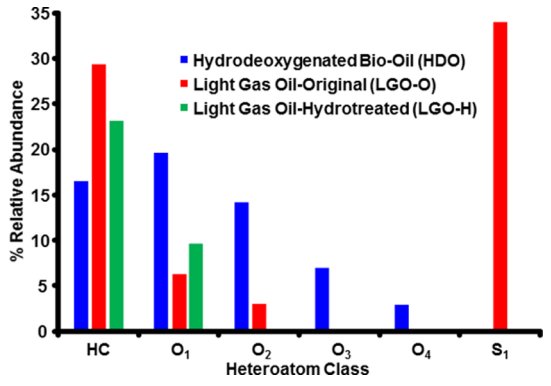

Figure 1. (+) APPI FT-ICR MS-derived heteroatom class distribution for the oil feeds used for blend production. O_x and S_x denote ions containing carbon, hydrogen, and x oxygen or sulfur atoms.

https://dx.doi.org/10.1021/acs.energyfuels.0c02437
Energy Fuels 2020, 34, 16181−16186

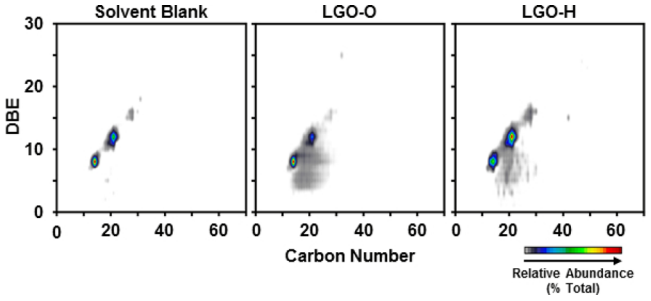

Figure 2. (+) APPI FT-ICR MS-derived isoabundance-contoured DBE vs carbon number plots for the O_1 heteroatom class from the oil feeds used for blend production and the solvent blank.

versus carbon number plots for the O_1 class from the solvent blank and the LGO. The compositional ranges of high relative abundance in the LGO are due to the peaks also seen in the solvent blank; however, the area of low-abundance O_1 species in gray are from the LGO. Because of the presence of these inseparable contaminant peaks, the relative abundances for the LGO O_x species are not representative of the actual abundance of oxygen in the sample and explain why the relative abundance for the LGO-H is greater than that for LGO-O.

Compositional coverage in the FT-ICR MS-derived DBE versus carbon number plots for the hydrocarbon class shows a wider range in carbon number and DBE for the HDO bio-oil than for the LGO (Figure 3). The areas of highest relative abundance (red) in the LGO-O are at DBE 4 and 8, corresponding to molecules with one and two aromatic rings, whereas the area of highest relative abundance in the LGO-H plot is only at DBE 4, indicating removal of aromatic rings during hydrotreatment. The oxygenated O_1 to O_4 species in the HDO bio-oil exhibit similar compositional coverage in their DBE versus carbon number plots, with wide ranges of carbon number and DBE (Figure 4). This wide range indicates hydrocarbon molecules with varying number of aromatic and nonaromatic rings with differing extents of alkylation.

FT-ICR MS of Blended Oil and Its Hydrotreatment. The HDO/LGO blend has characteristics similar to both individual feeds, the HDO bio-oil and LGO-O, illustrated in the heteroatom class graph, in which the O_1 and O_2 classes correlate with the HDO bio-oil, and the S_1 class correlates with the LGO-O (Figure 5). The S_1 heteroatom class from the LGO-O and the blend have the same compositional coverage in the DBE versus carbon number plots and contain molecules at high relative abundance at DBE 6 and 9, indicative of

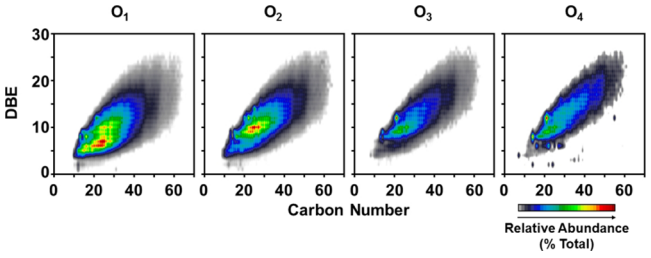

Figure 4. (+) APPI FT-ICR MS-derived isoabundance-contoured DBE vs carbon number plots for the O_1–O_4 heteroatom classes from the HDO bio-oil feed used for the blend production.

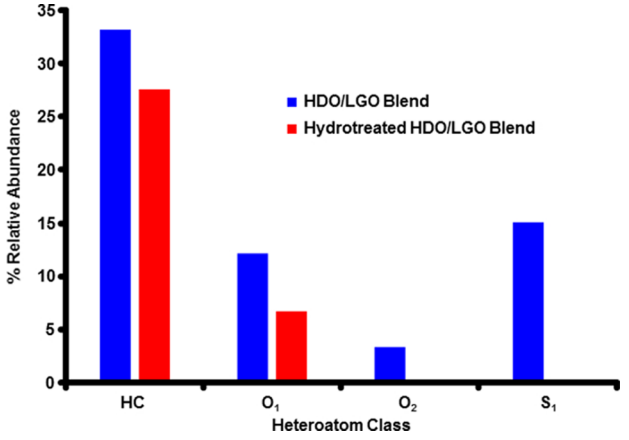

Figure 5. (+) APPI FT-ICR MS-derived heteroatom class distributions for the blend and hydroblend.

benzothiophenes (DBE 6) and dibenzothiophenes (DBE 9) (Figure 6). The compositional similarity between the LGO-O and blend S_1 class indicates that no major structural changes are caused by blending; however, the concentration of S_1 species is lower in the blend because of dilution of the LGO with the HDO bio-oil. The compositional coverage for the hydrocarbon class in the blend is similar to that for the HDO bio-oil. The area of highest relative abundance is closer to that for LGO-O (carbon number 10–30 and DBE 4–15) (Figure 7). Based on the S_1 class, the oxygen species in the blend have compositional coverage similar to that for their initial feed, the HDO bio-oil, but at lower concentration because of dilution during blending (Figure 8). The similarities between the blend and original feeds show that no major molecular transformations occur during blending.

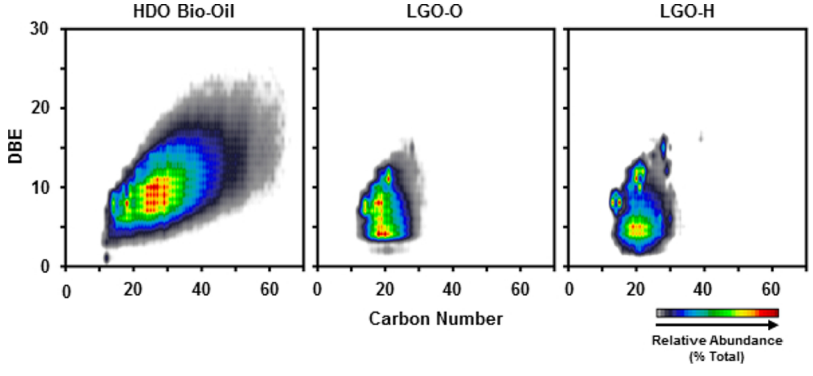

Figure 3. (+) APPI FT-ICR MS-derived isoabundance-contoured DBE vs carbon number plots for the hydrocarbon heteroatom class from the oil feeds used for blend production.

https://dx.doi.org/10.1021/acs.energyfuels.0c02437
Energy Fuels 2020, 34, 16181–16186

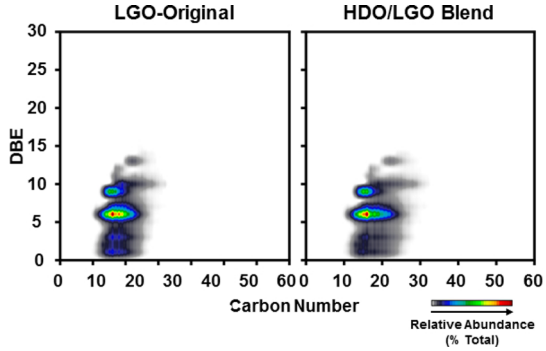

Figure 6. (+) APPI FT-ICR MS-derived isoabundance-contoured DBE vs carbon number plots for the S_1 heteroatom class from the LGO-O and the blend.

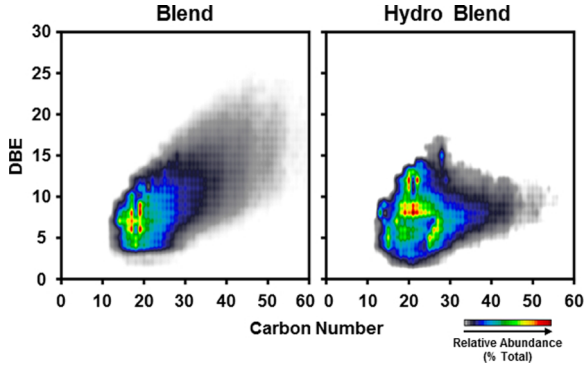

Figure 7. (+) APPI FT-ICR MS-derived isoabundance-contoured DBE vs carbon number plots for the hydrocarbon heteroatom class from the blend and the hydroblend.

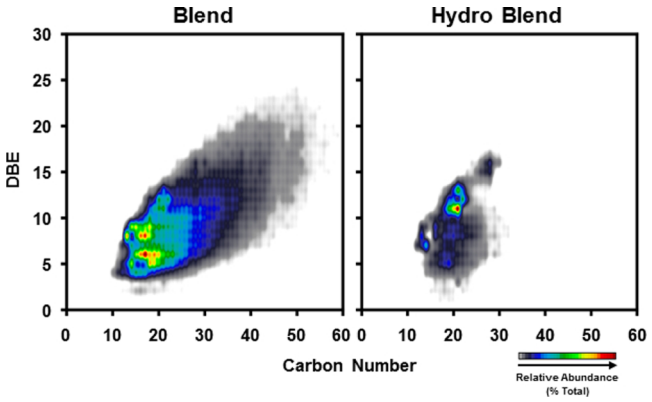

Figure 8. (+) APPI FT-ICR MS-derived isoabundance-contoured DBE vs carbon number plots for the O_1 heteroatom class from the blend and the hydroblend.

The effectiveness of hydrotreatment in removing both oxygen- and sulfur-containing species is seen in Figure 5, in which S_1 and O_2 are not present in the blended oil after hydrotreatment (hydroblend). As in Figure 1, the relative abundance of the O_1 class in the hydroblend is not representative of the actual abundance of oxygenated species because of peaks due to solvent contaminants; however, the compositional coverage in Figure 8 of the hydroblend after removal of the contaminant peaks does indicate O_1 species that are not removed during hydrotreatment. In Figure 7, the compositional range for the hydrocarbon class shows a slight reduction in the carbon number and DBE after hydrotreatment, with an abundance-weighted average of 23 carbons and a DBE of 9 for the blend and 22 carbons and a DBE of 8 for the hydroblend. A more significant difference between the blend and the hydroblend is the low-abundance species that have DBE greater than ~15, which are present in the blend and not in the hydroblend, corresponding to a reduction in large aromatic hydrocarbons that are associated with the formation of coke.[23] A reduction in the carbon number and DBE is also seen in the O_1 class on hydrotreatment, although the change is much more pronounced, with the maximum carbon number for the blend reduced from 60 to 30 and the DBE reduced from 25 to ~15 (Figure 8).

GCxGC Analysis of Blended Oil before and after Hydrotreatment. GCxGC MS provides for compound class identification and comparison of the blended oil and its hydrotreated counterpart (Figure 9). In these chromatograms, components from each feed were determined by subtraction of either the LGO-O or LGO-H from the blend and hydroblend. White peaks are more abundant in the LGO, and black peaks are more abundant in the blend/hydroblend. Species that are more abundant in the LGO mean that the corresponding component in the blend is from the LGO, and components that are not from the LGO are, therefore, from the HDO bio-oil. In the blend minus LGO-O chromatogram (Figure 9, top), the compounds contributed by the LGO-O are primarily alkanes and S-containing compounds and also include naphthalene and benzene derivatives. The components in the blend contributed by the HDO bio-oil are low-molecular-weight cycloalkanes, indene derivatives, phenols, and assorted aromatic hydrocarbons. The bottom chromatogram in Figure 9 shows the LGO-H subtracted from the hydroblend. In the bottom chromatogram, the alkanes are white, indicating a higher abundance in the LGO-H and therefore still attributed to the LGO feed. The black peaks are assigned to cycloalkanes from the HDO bio-oil. In the hydrotreated samples, the S- and O-containing compounds are not present, showing that they were successfully removed. Comparison of the two chromatograms shows that the compositional ranges attributed to either the HDO bio-oil or LGO are essentially the same, illustrating that the contributions from each feed remain the same throughout the blending and hydrotreating process. GCxGC MS results thus correlate with the trends seen by FT-ICR MS.

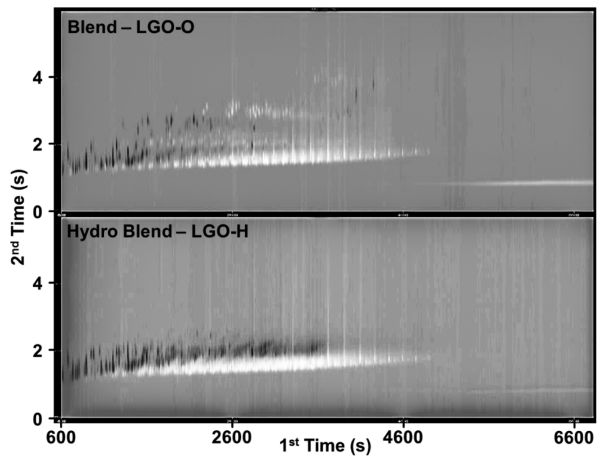

Figure 9. GCxGC MS difference chromatograms for the blend minus the LGO-O and the hydroblend minus the LGO-H.

https://dx.doi.org/10.1021/acs.energyfuels.0c02437
Energy Fuels 2020, 34, 16181−16186

CONCLUSIONS

Two complementary methods, FT-ICR MS and GCxGC MS, were utilized to track compositional changes of a hydrotreated crude bio-oil through blending with an LGO and subsequent hydrotreatment of the blend. Comparison of the hydrocarbons, oxygen, and sulfur heteroatom classes before and after blending revealed no compositional changes that result from blending; however, the sulfur and oxygen species were less abundant because of dilution. Hydrotreatment of the blend completely removed sulfur and all but a few O_1 species and resulted in the reduction of components with high DBE and carbon number for both hydrocarbon and oxygen classes. GCxGC MS identified compound classes that were contributed by each of the individual feeds and confirmed the results found by FT-ICR MS. The chromatograms for the blend and hydroblend minus their respective LGO showed that the alkanes are contributed by the LGO, whereas cycloalkanes are from the HDO bio-oil. Both feeds contributed aromatic components in the blend, with naphthalene from the LGO and indene derivatives and phenols from the HDO bio-oil.

AUTHOR INFORMATION

Corresponding Author

Steven M. Rowland − *Ion Cyclotron Resonance Program, National High Magnetic Field Laboratory and Future Fuels Institute, Florida State University, Tallahassee, Florida 32310, United States*; Phone: 303-275-4276; Email: steven.rowland@nrel.gov

Authors

Rebecca L. Ware − *Department of Chemistry and Biochemistry, Florida State University, Tallahassee, Florida 32306, United States*

Ryan P. Rodgers − *Ion Cyclotron Resonance Program, National High Magnetic Field Laboratory and Future Fuels Institute, Florida State University, Tallahassee, Florida 32310, United States*; orcid.org/0000-0003-1302-2850

Alan G. Marshall − *Department of Chemistry and Biochemistry and Ion Cyclotron Resonance Program, National High Magnetic Field Laboratory, Florida State University, Tallahassee, Florida 32306, United States*; orcid.org/0000-0001-9375-2532

Ofei D. Mante − *Technology Advancement and Commercialization, RTI International, Research Triangle Park, North Carolina 27709, United States*; orcid.org/0000-0002-0960-2943

David C. Dayton − *Technology Advancement and Commercialization, RTI International, Research Triangle Park, North Carolina 27709, United States*; orcid.org/0000-0003-3244-3722

Sylvain Verdier − *Haldor Topsoe A/S, DK-2800 Kgs. Lyngby, Denmark*

Jostein Gabrielsen − *Haldor Topsoe A/S, DK-2800 Kgs. Lyngby, Denmark*

Complete contact information is available at: https://pubs.acs.org/10.1021/acs.energyfuels.0c02437

Notes

The authors declare no competing financial interest.

ACKNOWLEDGMENTS

This work was supported by the NSF Division of Materials Research (DMR-1157490 and DMR-1644779) and the State of Florida. We thank Greg T. Blakney, Donald F. Smith, and John P. Quinn for continued assistance in instrument maintenance and data analysis. The authors also thank Yuri E. Corilo for providing data processing and imaging software.

REFERENCES

(1) Zacher, A. H.; Olarte, M. V.; Santosa, D. M.; Elliott, D. C.; Jones, S. B. A Review and Perspective of Recent Bio-Oil Hydrotreating Research. *Green Chem.* **2014**, *16*, 491−515.

(2) Krutof, A.; Hawboldt, K. Blends of Pyrolysis Oil, Petroleum, and Other Bio-Based Fuels: A Review. *Renew. Sustain. Energy Rev.* **2016**, *59*, 406−419.

(3) Weerachanchai, P.; Tangsathitkulchai, C.; Tangsathitkulchai, M. Phase Behaviors and Fuel Properties of Bio-Oil-Diesel-Alcohol Blends. *World Acad. Sci. Eng. Technol.* **2009**, *56*, 387−393.

(4) Ikura, M.; Stanciulescu, M.; Hogan, E. Emulsification of Pyrolysis Derived Bio-Oil in Diesel Fuel. *Biomass Bioenergy* **2003**, *24*, 221−232.

(5) Chiaramonti, D.; Bonini, M.; Fratini, E.; Tondi, G.; Gartner, K.; Bridgwater, A. V.; Grimm, H. P.; Soldaini, I.; Webster, A.; Baglioni, P. Development of emulsions from biomass pyrolysis liquid and diesel and their use in engines-Part 1 : emulsion production. *Biomass Bioenergy* **2003**, *25*, 85−99.

(6) de Luna, M. D. G.; Cruz, L. A. D.; Chen, W.-H.; Lin, B.-J.; Hsieh, T.-H. Improving the Stability of Diesel Emulsions with High Pyrolysis Bio-Oil Content by Alcohol Co-Surfactants and High Shear Mixing Strategies. *Energy* **2017**, *141*, 1416−1428.

(7) Martin, J. A.; Mullen, C. A.; Boateng, A. A. Maximizing the Stability of Pyrolysis Oil/Diesel Fuel Emulsions. *Energy Fuels* **2014**, *28*, 5918−5929.

(8) Jarvis, M. W.; Olstad, J.; Parent, Y.; Deutch, S.; Iisa, K.; Christensen, E.; Ben, H.; Black, S.; Nimlos, M.; Magrini, K. Catalytic Upgrading of Biomass Pyrolysis Oxygenates with Vacuum Gas Oil Using a Davison Circulating Riser Reactor. *Energy Fuels* **2018**, *32*, 1733−1743.

(9) Pinho, A. d. R.; de Almeida, M. B. B.; Mendes, F. L.; Casavechia, L. C.; Talmadge, M. S.; Kinchin, C. M.; Chum, H. L. Fast Pyrolysis Oil from Pinewood Chips Co-Processing with Vacuum Gas Oil in an FCC Unit for Second Generation Fuel Production. *Fuel* **2017**, *188*, 462−473.

(10) Huynh, T. M.; Armbruster, U.; Atia, H.; Bentrup, U.; Phan, B. M. Q.; Eckelt, R.; Nguyen, L. H.; Nguyen, D. A.; Martin, A. Upgrading of Bio-Oil and Subsequent Co-Processing under FCC Conditions for Fuel Production. *React. Chem. Eng.* **2016**, *1*, 239−251.

(11) Fogassy, G.; Thegarid, N.; Toussaint, G.; van Veen, A. C.; Schuurman, Y.; Mirodatos, C. Biomass Derived Feedstock Co-Processing with Vacuum Gas Oil for Second-Generation Fuel Production in FCC Units. *Appl. Catal., B* **2010**, *96*, 476−485.

(12) Fogassy, G.; Thegarid, N.; Schuurman, Y.; Mirodatos, C. From Biomass to Bio-Gasoline by FCC Co-Processing: Effect of Feed Composition and Catalyst Structure on Product Quality. *Energy Environ. Sci.* **2011**, *4*, 5068−5076.

(13) Ibarra, Á.; Rodríguez, E.; Sedran, U.; Arandes, J. M.; Bilbao, J. Synergy in the Cracking of a Blend of Bio-Oil and Vacuum Gasoil under Fluid Catalytic Cracking Conditions. *Ind. Eng. Chem. Res.* **2016**, *55*, 1872−1880.

(14) Ware, R. L.; Rodgers, R. P.; Marshall, A. G.; Mante, O. D.; Dayton, D. C.; Verdier, S.; Gabrielsen, J.; Rowland, S. M. Detailed Chemical Composition of an Oak Biocrude and Its Hydrotreated Product Determined by Positive Atmospheric Pressure Photoionization Fourier Transform Ion Cyclotron Resonance Mass Spectrometry. *Sustainable Energy Fuels* **2020**, *4*, 2404−2410.

(15) Mante, O. D.; Dayton, D. C.; Gabrielsen, J.; Ammitzboll, N. L.; Barbee, D.; Verdier, S.; Wang, K. Integration of Catalytic Fast Pyrolysis and Hydroprocessing: A Pathway to Refinery Intermediates

and "Drop-in" Fuels from Biomass. *Green Chem.* **2016**, *18*, 6123−6135.
(16) Ware, R. L.; Rowland, S. M.; Rodgers, R. P.; Marshall, A. G. Advanced Chemical Characterization of Pyrolysis Oils from Landfill Waste, Recycled Plastics, and Forestry Residue. *Energy Fuels* **2017**, *31*, 8210−8216.
(17) Kaiser, N. K.; Quinn, J. P.; Blakney, G. T.; Hendrickson, C. L.; Marshall, A. G. A Novel 9.4 Tesla FTICR Mass Spectrometer with Improved Sensitivity, Mass Resolution, and Mass Range. *J. Am. Soc. Mass Spectrom.* **2011**, *22*, 1343−1351.
(18) Blakney, G. T.; Hendrickson, C. L.; Marshall, A. G. Predator Data Station: A Fast Data Acquisition System for Advanced FT-ICR MS Experiments. *Int. J. Mass Spectrom.* **2011**, *306*, 246−252.
(19) Jarvis, J. M.; Page-dumroese, D. S.; Anderson, N. M.; Corilo, Y.; Rodgers, R. P. Characterization of Fast Pyrolysis Products Generated from Several Western USA Woody Species. *Energy Fuels* **2014**, *28*, 6438−6446.
(20) Marshall, A. G.; Hendrickson, C. L.; Jackson, G. S. Fourier transform ion cyclotron resonance mass spectrometry: A primer. *Mass Spectrom. Rev.* **1998**, *17*, 1−35.
(21) Xian, F.; Hendrickson, C. L.; Blakney, G. T.; Beu, S. C.; Marshall, A. G. Automated Broadband Phase Correction of Fourier Transform Ion Cyclotron Resonance Mass Spectra. *Anal. Chem.* **2010**, *82*, 8807−8812.
(22) *PetroOrg*; The Florida State University, All Rights Reserved, 2017.
(23) Furimsky, E.; Massoth, F. E. Deactivation of Hydroprocessing Catalysts. *Catal. Today* **1999**, *52*, 381−495.

https://dx.doi.org/10.1021/acs.energyfuels.0c02437
Energy Fuels 2020, 34, 16181−16186